Muon (g − 2) and XENON1T excess with boosted dark matter in L − L model

4 authors:

Debasish Borah
Indian Institute of Technology Guwahati
168 PUBLICATIONS   1,757 CITATIONS

SEE PROFILE

Manoranjan Dutta
Indian Institute of Technology Hyderabad
13 PUBLICATIONS   7 CITATIONS

SEE PROFILE

Satyabrata Mahapatra
Indian Institute of Technology Hyderabad
13 PUBLICATIONS   22 CITATIONS

SEE PROFILE

Narendra Sahu
Indian Institute of Technology Hyderabad
75 PUBLICATIONS   1,545 CITATIONS

SEE PROFILE

Some of the authors of this publication are also working on these related projects:

Verifiable Type-II seesaw and Dark matter in a gauged U(1)_{B-L} Model View project

Self-Interacting Dark matter View project

Muon $(g-2)$ and XENON1T Excess with Boosted Dark Matter in $L_\mu - L_\tau$ Model

Debasish Borah,[1, *] Manoranjan Dutta,[2, †] Satyabrata Mahapatra,[2, ‡] and Narendra Sahu[2, §]

¹Department of Physics, Indian Institute of Technology Guwahati, Assam 781039, India
²Department of Physics, Indian Institute of Technology Hyderabad,
Kandi, Sangareddy 502285, Telangana, India

Abstract

Motivated by the growing evidence for lepton flavour universality violation after the first results from Fermilab's muon $(g-2)$ measurement, we revisit one of the most widely studied anomaly free extensions of the standard model namely, gauged $L_\mu - L_\tau$ model, known to be providing a natural explanation for muon $(g-2)$. We also incorporate the presence of dark matter (DM) in this model in order to explain the recently reported electron recoil excess by the XENON1T collaboration. We show that the same neutral gauge boson responsible for generating the required muon $(g-2)$ can also mediate interactions between electron and dark fermions boosted by dark matter annihilation. The required DM annihilation rate into dark fermion require a hybrid setup of thermal and non-thermal mechanisms to generate DM relic density. The tightly constrained parameter space from all requirements remain sensitive to ongoing and near future experiments, keeping the scenario very predictive.

Introduction: The recent measurement of the muon anomalous magnetic moment, $a_\mu = (g-2)_\mu/2$, by the E989 experiment at Fermilab shows a discrepancy with respect to the theoretical prediction of the Standard Model (SM) [1]

$$a_\mu^{\text{FNAL}} = 116592040(54) \times 10^{-11} \quad (1)$$

$$a_\mu^{\text{SM}} = 116591810(43) \times 10^{-11} \quad (2)$$

which when combined with the previous Brookhaven determination of

$$a_\mu^{\text{BNL}} = 116592089(63) \times 10^{-11} \quad (3)$$

leads to a 4.2 σ observed excess of $\Delta a_\mu = 251(59) \times 10^{-11}$. The status of the SM calculation of muon magnetic moment has been updated recently in [2][1]. For more details, one may refer to [4–8]. The latest Fermilab measurements have also led to several recent works on updating possible theoretical models with new data. For example, see [9–15] for minimal dark matter (DM) motivated scenarios, [16–18] for axion like particle (ALP) motivated scenarios, [19, 20] for gauged lepton flavour models like $U(1)_{L_\mu-L_\tau}$ and [21–44] for other phenomenological scenarios like supersymmetry, multi-Higgs doublet models etc. and other implications of this new measurement. For a comprehensive review on new physics explanations of muon $(g-2)$ anomaly, please see [45]. Another evidence of such lepton flavour universality (LFU) violation, that too in the context of muon, comes from the measurement of $R_K = \text{BR}(B \to K\mu^+\mu^-)/\text{BR}(B \to Ke^+e^-)$. While the hint for this anomaly, like muon $(g-2)$ was there for several years, recent update from the LHCb collaboration [46] has led to the most precise measurement ever

with more than 3σ deviation from the SM predictions. In the light of growing evidences for such LFU violations, need for beyond standard model physics around the TeV corner has become very prominent.

Another recent anomaly is the one reported by the XENON1T collaboration in 2020 related to their observation of an excess of electron recoil events over the background in the recoil energy E_r in a range 1-7 keV, peaked around 2.4 keV[47]. Although solar axions and neutrinos with magnetic moment can explain the excess at 3.5σ and 3.2σ significance respectively, they are severely plagued by stellar cooling bounds. This has led to several interesting new physics explanations, see [48–68] and references therein. The DM interpretations out of these examples, typically have a light mediator via which DM interacts with electrons. The recoil can occur either due to light boosted DM or inelastic up or down-scattering [55–64, 68–78, 78–80].

Here we consider the popular and minimal model based on the gauged $L_\mu - L_\tau$ symmetry which is anomaly free [81, 82]. In earlier attempts to explain XENON1T excess with inelastic DM in gauged $L_\mu - L_\tau$ model [56] which can also explain $(g-2)_\mu$, only a tiny parameter space was allowed from all requirements even while considering a much larger error bars in $(g-2)_\mu$ namely $\Delta a_\mu = (27.9 \pm 22.8) \times 10^{-10}$, consistent with the 3.7σ discrepancy prior to the Fermilab measurement. As can be seen from [56], the main obstacle in satisfying both the excess is the constraint on heavier DM lifetime. To be more specific, in such scenarios, the heavier DM must be present in the universe at current epoch so that it can give rise to inelastic down-scattering at XENON1T detector. However, the same process responsible for such scattering also leads to heavier DM decay into lighter DM and SM particles leading to stringent constraints. Therefore, in this work, we consider a single component DM scenario which can annihilate into boosted lighter particles so that the latter can scatter off electron elastically, giving rise to the required excess. Boosted DM interpretation of XENON1T excess in the context of different models

---

[1] The latest lattice results [3] however, predict a larger value of muon $(g-2)$ bringing it closer to experimental value.

have been discussed in [50–53, 77, 78, 78–80] [2]. We study this possibility within the framework of gauged $L_\mu - L_\tau$ model along with the possibility of explaining the muon $(g-2)$ data. While we do not pursue the study of R_K anomalies in this model, one may refer to [85] for common origin of muon $(g-2)$ and R_K anomalies along with dark matter in extensions of minimal $L_\mu - L_\tau$ model.

Gauged $L_\mu - L_\tau$ Symmetry: The SM fermion content with their gauge charges under $SU(3)_c \times SU(2)_L \times U(1)_Y \times U(1)_{L_\mu - L_\tau}$ gauge symmetry are denoted as follows.

$$q_L = \begin{pmatrix} u_L \\ d_L \end{pmatrix} \sim (3, 2, \frac{1}{6}, 0),\ u_R(d_R) \sim (3, 1, \frac{2}{3}(-\frac{1}{3}), 0)$$

$$L_e = \begin{pmatrix} \nu_e \\ e_L \end{pmatrix} \sim (1, 2, -\frac{1}{2}, 0),\ e_R \sim (1, 1, -1, 0)$$

$$L_\mu = \begin{pmatrix} \nu_\mu \\ \mu_L \end{pmatrix} \sim (1, 2, -\frac{1}{2}, 1),\ \mu_R \sim (1, 1, -1, 1)$$

$$L_\tau = \begin{pmatrix} \nu_\tau \\ \tau_L \end{pmatrix} \sim (1, 2, -\frac{1}{2}, -1),\ \tau_R \sim (1, 1, -1, -1)$$

Three right handed neutrinos N_e, N_μ, N_τ with $L_\mu - L_\tau$ charges $0, 1, -1$ respectively can be introduced along with singlet scalars Φ_1, Φ_2 with corresponding $L_\mu - L_\tau$ charges $1, -1$ respectively to take care of spontaneous gauge symmetry breaking and type I seesaw origin of light neutrino masses (see [86] and references therein for details). Denoting the vacuum expectation values (VEV) of singlets $\Phi_{1,2}$ as $v_{1,2}$, the new gauge boson mass can be found to be $M_{Z'} = g_{\mu\tau} \sqrt{(v_1^2 + v_2^2)}$ with $g_{\mu\tau}$ being the $L_\mu - L_\tau$ gauge coupling. Clearly the model predicts diagonal charged lepton mass matrix M_ℓ and diagonal Dirac Yukawa of light neutrinos. Thus, the non-trivial neutrino mixing will arise from the structure of right handed neutrino mass matrix M_R only which is generated by the chosen scalar singlet fields.

For dark matter sector, we introduce two additional vector like fermions $\psi_{A,B}$ and two additional singlet scalar η and ξ. The $L_\mu - L_\tau$ gauge couplings of $\psi_A, \psi_B, \eta, \xi$ are taken to be $0, g_B, 0$ and 0 respectively. While η gives rise to non-thermal contribution to ψ_A abundance via late decay, the other scalar ξ is responsible for mediating ψ_A annihilation into ψ_B. The relevant Lagrangian can be written as follows.

$$\mathcal{L} \supseteq \overline{\psi_A} i\gamma^\mu \partial_\mu \psi_A - m_A \overline{\psi_A} \psi_A + \overline{\psi_B} i\gamma^\mu D_\mu \psi_B - m_B \overline{\psi_B} \psi_B - y_A \eta \overline{\psi_A} \psi_A - y_B \eta \overline{\psi_B} \psi_B - y_1 \xi \overline{\psi_A} \psi_A - y_2 \xi \overline{\psi_B} \psi_B + \text{h.c.}$$ (4)

---

[2] See [83, 84] for earlier works on this possibility.

Here $D_\mu \psi_B = (\partial_\mu - ig_B Z'_\mu) \psi_B$. Here $g_B = n_B g_{\mu\tau}$ with n_B being gauge charge of vector like fermion ψ_B. Since n_B can be chosen independently, we keep g_B as a free parameter. For simplicity, we take $y_B = 0$ whereas y_A is taken to be very small to realise the desired DM phenomenology to be discussed later. Since the scalar singlet η is required to be produced in thermal bath leaving a thermal relic followed by late decay into DM (to be discussed below), we also write down its key interactions as

$$-\mathcal{L}_\eta \supset \lambda_\eta \eta^4 + \lambda_{\eta H} \eta^2 (H_1^\dagger H_1) + \lambda_{\eta \Phi_1} \eta^2 (\Phi_1^\dagger \Phi_1) + \lambda_{\eta \Phi_2} \eta^2 (\Phi_2^\dagger \Phi_2) + \lambda_{\eta \xi} \eta^2 \xi^2$$ (5)

where H_1 denotes the SM Higgs field.

It should be noted that, a kinetic mixing term between $U(1)_Y$ of SM and $U(1)_{L_\mu - L_\tau}$ of the form $\frac{\epsilon}{2} B^{\alpha\beta} Y_{\alpha\beta}$ can exist in the Lagrangian where $B^{\alpha\beta} = \partial^\alpha X^\beta - \partial^\beta X^\alpha, Y_{\alpha\beta}$ are the field strength tensors of $U(1)_{L_\mu - L_\tau}, U(1)_Y$ respectively and ϵ is the mixing parameter. Even if this mixing is considered to be absent in the Lagrangian, it can arise at one loop level with particles charged under both the gauge sectors in the loop. We consider this mixing to be $\epsilon = g_{\mu\tau}/70$. While the phenomenology of muon $(g-2)$, and DM relic in our model is not dependent on this mixing, the XENON1T fit as well as other experimental constraints on the model parameters can crucially depend upon this mixing. We therefore choose it to be small, around the same order as its one loop value.

Anomalous Muon Magnetic Moment: The magnetic moment of muon is given by

$$\overrightarrow{\mu_\mu} = g_\mu \left(\frac{q}{2m} \right) \overrightarrow{S},$$ (6)

where g_μ is the gyromagnetic ratio and its value is 2 for a structureless, spin $\frac{1}{2}$ particle of mass m and charge q. Any radiative correction, which couples the muon spin to the virtual fields, contributes to its magnetic moment and is given by

$$a_\mu = \frac{1}{2}(g_\mu - 2)$$ (7)

The anomalous muon magnetic moment has been measured very precisely while it has also been predicted in the SM to a great accuracy. In our model, the additional contribution to muon magnetic moment comes from one loop diagram mediated by Z' boson. The contribution is given by [87–89]

$$\Delta a_\mu = \frac{\alpha'}{2\pi} \int_0^1 dx \frac{2m_\mu^2 x^2 (1-x)}{x^2 m_\mu^2 + (1-x) M_{Z'}^2} \approx \frac{\alpha'}{2\pi} \frac{2m_\mu^2}{3M_{Z'}^2}$$ (8)

where $\alpha' = g_{\mu\tau}^2/(4\pi)$.

Relic Abundance of DM: Among the dark sector particles, we consider ψ_A to be the dominant DM candidate whose thermal relic is dictated by its annihilation

cross section into a pair of ψ_B. The scalar singlet η is also thermally produced but long lived and it decays at late epochs to ψ_A giving a non-thermal relic contribution. Since η coupling to ψ_A is very small from such late decay criteria, it relies upon scalar portal couplings to enter thermal equilibrium with the bath, similar to scalar singlet DM. With these in mind, we can now write down the Boltzmann equations for the DM candidate ψ_A along with ψ_B and the scalar singlet η whose late decays into DM is crucial to generate correct DM relic. Both the DM and the scalar singlet were in thermal equilibrium in the early universe. Due to large annihilation cross-section $\sigma(\psi_A \psi_A \to \psi_B \psi_B)$, the thermal freeze-out relic of DM is several orders of magnitude smaller than the observed relic density. However the relic can be lifted up to the correct ballpark from late decays of the scalar η into DM. The abundance of ψ_B is naturally suppressed due to its large interaction rate with $L_\mu - L_\tau$ gauge sector. For earlier works on interplay of $\psi_A \psi_A \to \psi_B \psi_B$ and $\psi_B \psi_B \to$ SM SM one may refer to [90]. We define comoving number densities of these particles as $Y_{\psi_A} = n_{\psi_A}/s, Y_{\psi_B} = n_{\psi_B}/s$ and $Y_\eta = n_\eta/s$. The relevant coupled Boltzmann equations can then be written as

$$
\frac{dY_{\psi_A}}{dx} = -\frac{s(m_A)}{x^2 H(m_A)}\langle\sigma(\psi_A\psi_A \to \psi_B\psi_B)v\rangle\left(Y_{\psi_A}^2 - \frac{(Y_{\psi_A}^{\rm eq})^2}{(Y_{\psi_B}^{\rm eq})^2}Y_{\psi_B}^2\right) - \frac{s(m_A)}{x^2 H(m_A)}\langle\sigma(\psi_A\psi_A \to \xi\xi)v\rangle\left(Y_{\psi_A}^2 - (Y_{\psi_A}^{\rm eq})^2\right)
$$

$$
+ \frac{2x}{H(m_A)}\left(\langle\Gamma_{\eta\to\psi_A\psi_A}\rangle Y_\eta\right)
$$

$$
\frac{dY_{\psi_B}}{dx} = +\frac{s(m_A)}{x^2 H(m_A)}\langle\sigma(\psi_A\psi_A \to \psi_B\psi_B)v\rangle\left(Y_{\psi_A}^2 - \frac{(Y_{\psi_A}^{\rm eq})^2}{(Y_{\psi_B}^{\rm eq})^2}Y_{\psi_B}^2\right) - \frac{s(m_A)}{x^2 H(m_A)}\langle\sigma(\psi_B\psi_B \to PP)v\rangle\left(Y_{\psi_B}^2 - (Y_{\psi_B}^{\rm eq})^2\right)
$$

$$
- \frac{s(m_A)}{x^2 H(m_A)}\langle\sigma(\psi_B\psi_B \to {\rm SM\ SM})v\rangle\left(Y_{\psi_B}^2 - (Y_{\psi_B}^{\rm eq})^2\right)
$$

$$
\frac{dY_\eta}{dx} = -\frac{s(m_A)}{x^2 H(m_A)}\langle\sigma(\eta\eta \to XX)v\rangle\left(Y_\eta^2 - (Y_\eta^{\rm eq})^2\right) - \frac{2x}{H(m_A)}\left(\langle\Gamma_{\eta\to\psi_A\psi_A}\rangle Y_\eta\right)
$$

where, $x = \frac{m_A}{T}$, $s(m_A) = \frac{2\pi^2}{45}g_{*s}m_A^3$ and $H(m_A) = 1.67 g_*^{1/2}\frac{m_A^2}{M_{Pl}}$. We show a benchmark plot in figure 1 with $m_\eta = 1$ GeV, $y_A = 10^{-10}$, $m_A = 0.1$ GeV, $m_B = 0.099875$ GeV, $M_{Z'} = 0.01$ GeV. We consider a large $\sigma(\psi_A\psi_A \to \psi_B\psi_B)$ cross section due to resonance enhancement $2m_A = m_\xi$. The reason behind choosing such a large cross section $\sigma(\psi_A\psi_A \to \psi_B\psi_B)$ will become clear when we discuss the XENON1T fit. Here, we have kept $\sigma(\psi_A\psi_A \to \psi_B\psi_B), \sigma(\eta\eta \to XX)$ as free parameters (within unitarity limits) and adjust them to achieve the desired XENON1T fit and DM relic. For example, the relevant couplings can be adjusted to realise such cross sections. All these relevant cross-sections and decay widths are given in the Appendix A. Note that the decay width $\Gamma_{\eta\to\psi_A\psi_A}$ is assumed to be very small leading to conversion of η into DM during the epoch of the big bang nucleosynthesis (BBN), but well before recombination. In fact, the chosen decay ($\Gamma_\eta = 3.7 \times 10^{-22}$ GeV) corresponds to a lifetime of approximately 1.7×10^{-3} s. This can be still safe from cosmological point of view by forbidding η decay into visible sector particles [91]. In figure 1, the dashed brown coloured line shows the equilibrium number density of the singlet scalar η. This singlet scalar was initially in thermal equilibrium with the SM bath. As its interaction rates falls below the expansion rate, it freezes out leaving a thermal relic, shown by the cyan dotted line. The DM particles $\psi_{A,B}$ were also in thermal equilibrium initially and their equilibrium number densities are shown by the green dashed line (they overlap due to very similar masses). As its interaction rate falls below Hubble rate of expansion, thermal freeze-out occurs leading to abundance of ψ_A several orders of magnitude smaller than the observed relic because of its large annihilation cross-section to ψ_B. This is shown by the purple dot-dashed line. The corresponding thermal freeze-out abundance of ψ_B is also suppressed because of its dominant annihilation into $Z'Z'$ which is shown by the orange dashed line. The blue dot dashed line depicts the evolution of comoving number density of ψ_A after considering the non-thermal contribution from η decay. The corresponding depletion of the η number density is shown by the red coloured dashed line. Clearly, as the number density of the scalar falls due to its decay, the DM number density gets uplifted. As the comoving number density of ψ_A increases, it again starts to annihilate into $\psi_B\psi_B$, leading to depletion in ψ_A density. Therefore, the final abundance of ψ_B which is shown by the dashed pink coloured line, is the result of its production from $\psi_A\psi_A$ annihilation and its depletion through $\psi_B\psi_B \to Z'Z'$. Clearly, even though the final abundance of ψ_B is suppressed, the correct relic of ψ_A can be obtained by appropriate tuning of the scalar decay width.
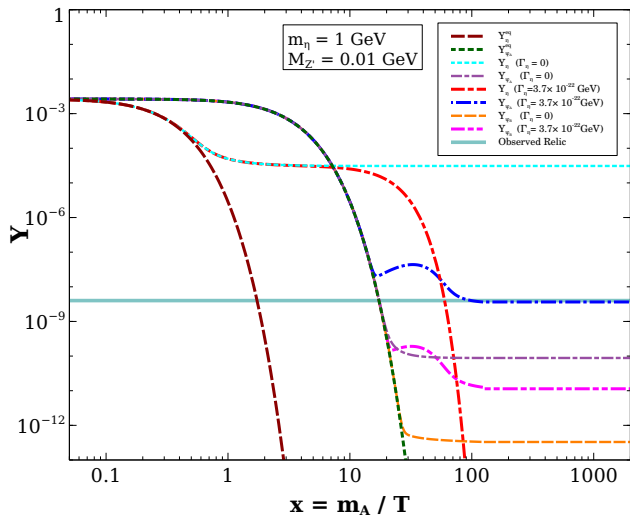
3

FIG. 1: Comoving number densities of DM candidates $\psi_{A,B}$ and long-lived scalar singlet η. The value of $\sigma(\eta\eta \to XX)$ used in the calculation is $1.45 \times 10^{-12} \text{GeV}^{-2}$ which can be obtained for $m_\eta = 1$ GeV, $m_X = 0.2$ GeV and the corresponding coupling 10^{-5} in Eq.A5

XENON1T Excess: As mentioned before, we adopt the boosted DM approach in order to explain the XENON1T excess. In this scenario, DM ψ_A annihilates into dark fermion ψ_B giving a significant boost to explain the reported excess in the electron recoil events at XENON1T experiment. For a fixed incoming velocity v of dark fermion, the differential scattering cross-section for the elastic scattering process $\psi_B e \to \psi_B e$ (with electrons inside the Xenon atom) can be written as

$$\frac{d\langle\sigma v\rangle}{dE_r} = \frac{\sigma_e}{2m_e v}\int_{q-}^{q+} a_0^2 q dq |F(q)|^2 K(E_r, q)\,, \quad (9)$$

where m_e is the electron mass, σ_e is the corresponding free electron cross section at fixed momentum transfer $q = 1/a_0$ with $a_0 = \frac{1}{\alpha m_e}$ being the Bohr radius, $\alpha = \frac{e^2}{4\pi} = \frac{1}{137}$ being the fine structure constant, E_r is the recoil energy of electron and $K(E_r, q)$ is the atomic excitation factor. For our calculations, the atomic excitation factor is adopted from [92] and we assume the dark fermion form factor to be unity. The dependency of atomic excitation factor on the transferred momentum q is shown in figure 2. Here the dominant contribution comes from the bound states with principal quantum number $n = 3$ as their binding energy is around a few keVs.

The free electron scattering cross-section for the process $\psi_B e \to \psi_B e$ is given by

$$\sigma_e = \frac{g_B^2 \epsilon^2 g^2 m_e^2}{\pi M_{Z'}^4} \quad (10)$$

ϵ is the kinetic mixing parameter between Z and Z' gauge bosons, g is the weak gauge coupling and g_B is the gauge

coupling between Z' and ψ_B defined earlier. It should be noted here that, for GeV scale dark fermion, σ_e is independent of ψ_B mass as the reduced mass of ψ_B-electron is almost equal to electron mass. For this elastic scattering the limits of integration are determined from the kinematics and are given by

$$q_\pm = m_B v \pm \sqrt{m_B^2 v^2 - 2m_B E_r}\,. \quad (11)$$

The differential event rate for the scattering of ψ_B with electrons in Xenon atom at XENON1T detector, i.e $\psi_B e \to \psi_B e$, can be written as

$$\frac{dR}{dE_r} = n_T \Phi_{\psi_B}\frac{d\langle\sigma v\rangle}{dE_r} \quad (12)$$

where $n_T = 4 \times 10^{27}$ Ton^{-1} is the number density of Xenon atoms and Φ_{ψ_B} is the flux of the boosted ψ_B particle.
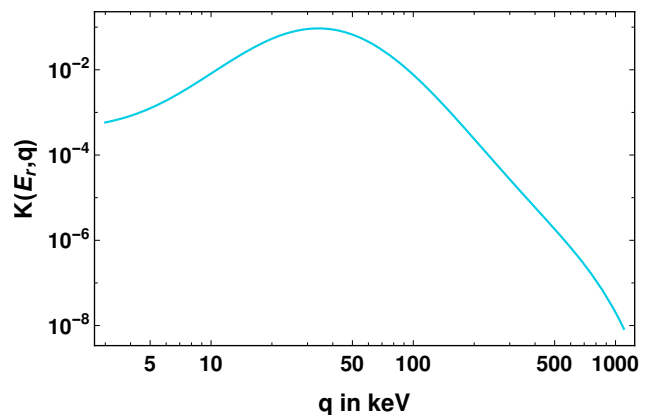

FIG. 2: Atomic excitation factor is shown as a function of momentum transferred.

Here we consider a scenario with two particles ψ_A and ψ_B where ψ_A is the dominant DM component in the present universe and it's annihilation in DM dense regions like the Galactic center (GC) or the Sun produces boosted ψ_B particles with the boost determined by the mass difference between ψ_A and ψ_B.

If one considers the GC to be the source of boosted dark fermion (via the annihilation of the DM with annihilation cross-section of order $\mathcal{O}(10^{-29} \text{ cm}^2)$, then the obtained flux is

$$\Phi_{\psi_B}^{\text{GC}} = 1.6 \times 10^5 \text{ cm}^{-2}\text{s}^{-1}\left(\frac{\langle\sigma_{\psi_A\psi_A \to \psi_B\psi_B}v\rangle}{10^{-29} \text{ cm}^2}\right)\left(\frac{0.1 \text{ GeV}}{m_A}\right)^2 \quad (13)$$

The detected recoil energy spectrum can be obtained by convolving Eq. (12) with the energy resolution of the XENON1T detector. Incorporating the detector efficiency $\gamma(E)$, the energy resolution of the detector is given by a Gaussian distribution with an energy dependent width,

$$\zeta(E, E_r) = \frac{1}{\sqrt{2\pi\sigma_{\text{det}}^2}}\text{Exp}\left[-\frac{(E - E_r)^2}{2\sigma_{\text{det}}^2}\right] \times \gamma(E) \quad (14)$$

4

where $\gamma(E)$ is reported in figure 2 of [47] and the width $\sigma_{\det}$ is given by

$$\sigma_{\det}(E) = a\sqrt{E} + bE \qquad (15)$$

with $a = 0.3171$ and $b = 0.0037$. Thus the final detected recoil energy spectrum is given by

$$\frac{dR_{\det}}{dE_r} = \frac{n_T \Phi_{\psi_B} \sigma_e a_0^2}{2m_e v} \int dE \ \zeta(E, E_r) \left[\int_{q-}^{q+} dq \ q K(E_r, q) \right] \qquad (16)$$

With the flux mentioned in Eq.(13), the electron scattering cross-section σ_e that can explain the electron recoil excess at XENON1T is calculated to be $7.2 \times 10^{-11} \mathrm{GeV}^{-2}$. To obtain the fit to XENON1T data
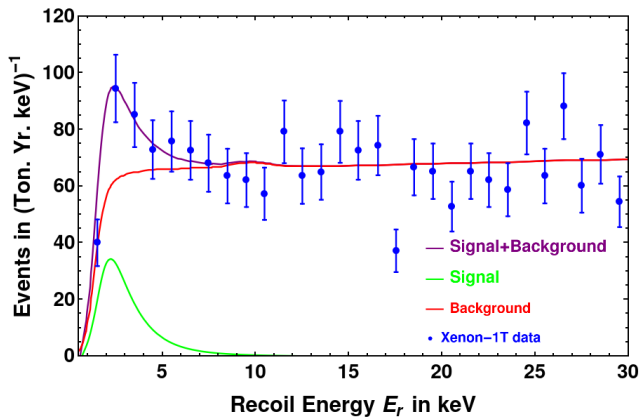

FIG. 3: Fit to XENON1T electron recoil excess with the Boosted dark fermion in $L_\mu - L_\tau$ model.
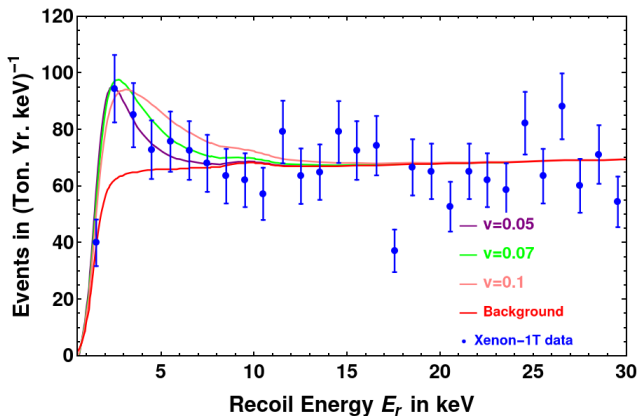

FIG. 4: Fit to XENON1T electron recoil excess with different velocity of the boosted dark fermion.

shown in figure 3 we have used benchmark values $m_B = 0.099875$ GeV, $v = 0.05$. Such velocities can be obtained by fixing $\Delta m / m_B = 1.25 \times 10^{-3}$ where $\Delta m = m_A - m_B$ giving rise to the necessary boost factor. In particular we have used In figure 4, we show the impact of different

dark fermion velocities on the fit. Clearly, higher velocities of dark fermion lead to flattening of the fit.

Note that there exists another possibility of getting boosted dark fermion flux from DM annihilation in the Sun. As DM particles can scatter off nuclei inside the Sun and hence gets captured by the Sun, then over certain period of time, DM can get accumulated at the Sun's core. Annihilation of these solar captured DM particles can, in principle, produce lighter boosted particles. In such a scenario the boosted DM flux is no longer dependent on the DM annihilation cross-section but rather it is fully determined by the DM capture rate which is characterised by the DM-nucleon scattering cross-section [51]. However, in order to avoid the evaporation bound of a few GeV for DM mass [93, 94], we need to choose DM mass in the GeV regime where DM-nucleon scattering rate faces tight constraints from direct search experiments like CRESST-III [95]. Therefore, one can not get the required enhancement in dark fermion flux from solar captured DM. This justifies the choice of GC as the origin of such DM annihilation into dark fermions.
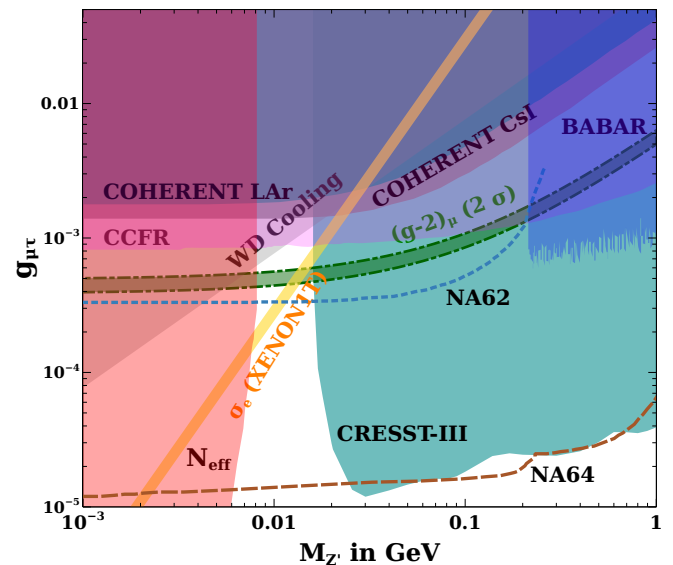
Conclusion:

FIG. 5: Summary plot showing the final parameter space allowed by all relevant constraints.

We summarize our result in figure 5 in terms of parameter space $g_{\mu\tau} - M_{Z'}$ with kinetic mixing parameter $\epsilon = g_{\mu\tau}/70$. The parameter space satisfying Fermilab's muon $(g-2)$ data is shown by the green coloured band. The orange solid band corresponds to $\sigma_e(\psi_B e \to \psi_B e) = (6.7 - 7.7) \times 10^{-11} \ \mathrm{GeV}^{-2}$ required to fit the XENON1T excess for the ψ_B velocity 0.05 and mass of 0.1 GeV.

Several experimental constraints are also shown as exclusion bands in the same summary plot of figure 5. The strongest constraint ruling out more than half of the $g_{\mu\tau} - M_{Z'}$ plane in figure 5 comes from low mass DM di-
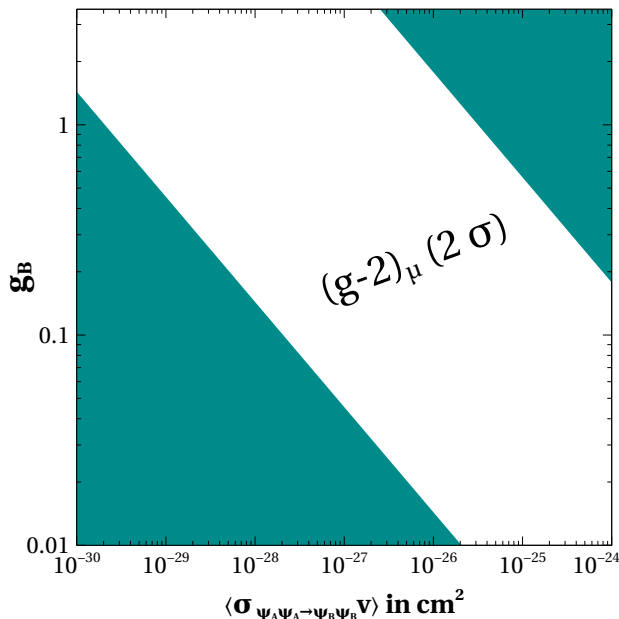
FIG. 6: Summary plot showing the final parameter space allowed by all relevant constraints in g_B versus $\sigma_{\psi_A\psi_A\to\psi_B\psi_B}v$ plane.

rect detection experiment CRESST-III [95], shown by the green shaded patch. The bound is severe due to the fact that boosted DM ψ_B interacts much more strongly with nucleons via Z' compared to other particles charged under $U(1)_{L_\mu-L_\tau}$ gauge symmetry. The pink shaded region corresponds to the parameter space excluded by upper bound on cross sections for $\nu N \to \nu N \mu\bar{\mu}$ measured by CCFR [96]. It completely rules out the parameter space satisfying $(g-2)_\mu$ beyond $M_{Z'} \gtrsim 0.2$ GeV. The observation of coherent elastic neutrino-nucleus cross section (CEνNS) in liquid argon (LAr) and cesium-iodide (CsI) performed by the COHERENT Collaboration [97, 98] also leads to constraint on $g_{\mu\tau} - M_{Z'}$ parameter space. Adopting the analysis of [99, 100], we show the constraints from COHERENT LAr and COHERENT CsI by the gray shaded regions. These experiments puts bounds on the CEνNS cross-section and hence constrains the corresponding coupling and the mediator mass. In the relatively high mass regime of Z', the constraint from the BABAR observations for 4μ final states [101], rules out the parameter space satisfying muon (g-2) beyond $M_{Z'} \gtrsim 0.2$ GeV similar to CCFR as shown by the blue shaded region. The astrophysical bounds from cooling of white dwarf (WD) [102, 103] excludes the upper left triangular region. Very light Z' is ruled out from cosmological constraints on effective relativistic degrees of freedom [103–106]. This arises due to the late decay of such light gauge bosons into SM leptons, after standard neutrino

decoupling temperatures thereby enhancing N_{eff}. Similar bound also exists for thermal DM masses in this regime which can annihilate into leptons. As shown by the authors of [107], such constraints from the BBN as well as the cosmic microwave background (CMB) measurements can be satisfied if $M_{\text{DM}} \gtrsim \mathcal{O}(1 \text{ MeV})$. While in our model we do have some late time annihilations of DM, as seen from figure 1, such annihilations are from dominant DM candidate ψ_A into sub-dominant DM candidate ψ_B without involving any visible sector particles in the final state, keeping the scenario safe from BBN bounds. On the other hand, the mass of singlet scalar ξ is kept at $2m_A$ for resonance enhancement of $\psi_A\psi_A \to \psi_B\psi_B$ cross section and hence heavy enough not to affect BBN.

We also checked that future experiments at CERN like NA62 [108] (blue dashed line of figure 5), and NA64 [109, 110] (brown dashed line in figure 5) is sensitive to our parameter space favoured from DM and muon $(g-2)$ requirements. Clearly, even after incorporating all existing experimental bounds, there still exists a small parameter space between a few MeV to around 100 MeV consistent with all bounds and the requirement of explaining muon $(g-2)$ and XENON1T excess. Using this final allowed region of parameter space in $g_{\mu\tau}-M_{Z'}$ plane from $(g-2)_\mu$ criteria, we show the dark sector parameter space in g_B versus $\sigma_{\psi_A\psi_A\to\psi_B\psi_B}v$ plane in figure 6. The white colored region is favoured by the latest $(g-2)_\mu$ data. The other parameters fixed are $m_A \approx m_B = 0.1$ GeV. Clearly, smaller is the annihilation cross section, smaller is the boosted fermion flux and larger is the required coupling g_B to give rise to the XENON1T fit.

Thus, the minimal model we study here is very much constrained from the requirement of $(g-2)_\mu$ as well as XENON1T excess from boosted DM. Both visible and dark sector parameters are tightly constrained to a narrow band from these requirements. This is clearly visible from the thin allowed region in figure 5. Future data from ongoing and near future experiments can probe the entire parameter space of this minimal and very predictive model.

Acknowledgments

6

APPENDIX A: RELEVANT CROSS-SECTION AND DECAY WIDTH

$$\Gamma(\eta \to \psi_A \psi_A) \;=\; \frac{y_A^2}{8\pi} m_\eta \Big(1 - 4\frac{m_A^2}{m_\eta^2}\Big)^{3/2} \tag{A1}$$

$$\sigma(\psi_A \psi_A \to \psi_B \psi_B) \;=\; \frac{y_1^2 y_2^2}{32\pi s} \frac{(s-4m_B^2)^{3/2}(s-4m_A^2)^{1/2}}{(s-m_\xi^2)^2} \tag{A2}$$

$$\sigma(\psi_{\rm B}\,\psi_{\rm B} \to Z'Z') \;=\; \frac{g_B'^4}{192\pi s(s-4m_B^2)} \times \left[\frac{24s(4m_B^4 + 2M_{Z'}^4 + sm_B^2)C}{M_{Z'}^4 + m_B^2 s - 4M_{Z'}^2 m_B^2} \right.$$
$$\left. -\; \frac{24(8m_B^2 - 4M_{Z'}^2 - s^2 - (s-2M_{Z'}^2)4m_B^2)}{s - 2M_{Z'}^2} \mathrm{Log}\Big[\frac{2M_{Z'}^2 + s(C-1)}{2M_{Z'}^2 - s(C+1)}\Big] \right] \tag{A3}$$

where $C = \sqrt{\frac{(s-4M_{Z'}^2)(s-4M_{\psi_1}^2)}{s^2}}$

$$\sigma(\psi_{A,B}\psi_{A,B} \to \xi\xi) \;=\; \frac{y_{1,2}^4}{32\pi s(s-4m_\psi^2)} \times \left[\frac{(3m_\xi^2 - 16m_\xi^2 m_\psi^2 + 16m_p^4 si - 2m_\psi^2 s)D}{m_\xi^4 - 2m_\xi^2 m_\psi^2 + sm_\psi^2} \right.$$
$$\left. -\; \frac{6m_\xi^4 - 32m_\psi^4 + 16m_\psi^2 s - 4m_\xi^2 s + 16m_\xi^2 m_\psi^2 + s^2}{s - 2m_\xi^2} Log\Big[\frac{2m_\xi^2 + D - s}{2m_\xi^2 - D - s}\Big] \right] \tag{A4}$$

where $D = \sqrt{(s-4m_\xi^2)(s-4m_\psi^2)}$

$$\sigma(\eta\eta \to \zeta\zeta) = \frac{\lambda_{\eta\zeta}^2}{64\pi s}\sqrt{\frac{s-4m_\zeta^2}{s-4m_\eta^2}} \tag{A5}$$

where ζ is any of the singlet scalar lighter than η.

Thermal averaged cross-section for annihilation of any particle A to B is given by: [111]

$$\langle \sigma v \rangle_{AA \to BB} = \frac{x}{2\big[K_1^2(x) + K_2^2(x)\big]} \times \int_2^\infty dz \sigma_{(AA \to BB)}(z^2 m_A^2)(z^2-4)z^2 K_1(zx) \tag{A6}$$

where $z = \sqrt{s}/m_A$ and $x = m_A/T$.

Thermal averaged decay width of η decaying to ψ_A is given by:

$$\langle \Gamma(\eta \to \psi_A \psi_A) \rangle = \Gamma(\eta \to \psi_A \psi_A)\left(\frac{K_1(x)}{K_2(x)}\right) \tag{A7}$$

In Eq. A6 and A7, K_1 and K_2 are the modified Bessel functions of 1st and 2nd kind respectively.

[1] B. Abi et al. (Muon g-2), Phys. Rev. Lett. **126**, 141801 (2021), 2104.03281.
[2] T. Aoyama et al. (2020), 2006.04822.
[3] S. Borsanyi et al. (2020), 2002.12347.
[4] P. A. Zyla et al. (Particle Data Group), PTEP **2020**, 083C01 (2020).
[5] M. Lindner, M. Platscher, and F. S. Queiroz, Phys. Rept. **731**, 1 (2018), 1610.06587.
[6] M. Davier, A. Hoecker, B. Malaescu, and Z. Zhang, Eur. Phys. J. C **80**, 241 (2020), [Erratum: Eur.Phys.J.C 80, 410 (2020)], 1908.00921.
[7] M. Davier, A. Hoecker, B. Malaescu, and Z. Zhang, Eur. Phys. J. C **77**, 827 (2017), 1706.09436.
[8] M. Davier, A. Hoecker, B. Malaescu, and Z. Zhang, Eur. Phys. J. C **71**, 1515 (2011), [Erratum: Eur.Phys.J.C 72, 1874 (2012)], 1010.4180.

[9] G. Arcadi, L. Calibbi, M. Fedele, and F. Mescia (2021), 2104.03228.

[10] B. Zhu and X. Liu (2021), 2104.03238.

[11] X.-F. Han, T. Li, H.-X. Wang, L. Wang, and Y. Zhang (2021), 2104.03227.

[12] S. Baum, M. Carena, N. R. Shah, and C. E. M. Wagner (2021), 2104.03302.

[13] Y. Bai and J. Berger (2021), 2104.03301.

[14] P. Das, M. Kumar Das, and N. Khan (2021), 2104.03271.

[15] C.-T. Lu, R. Ramos, and Y.-L. Sming Tsai (2021), 2104.04503.

[16] S.-F. Ge, X.-D. Ma, and P. Pasquini (2021), 2104.03276.

[17] V. Brdar, S. Jana, J. Kubo, and M. Lindner (2021), 2104.03282.

[18] M. A. Buen-Abad, J. Fan, M. Reece, and C. Sun (2021), 2104.03267.

[19] L. Zu, X. Pan, L. Feng, Q. Yuan, and Y.-Z. Fan (2021), 2104.03340.

[20] D. W. P. Amaral, D. G. Cerdeño, A. Cheek, and P. Foldenauer (2021), 2104.03297.

[21] M. Endo, K. Hamaguchi, S. Iwamoto, and T. Kitahara (2021), 2104.03217.

[22] W. Ahmed, I. Khan, J. Li, T. Li, S. Raza, and W. Zhang (2021), 2104.03491.

[23] M. Abdughani, Y.-Z. Fan, L. Feng, Y.-L. Sming Tsai, L. Wu, and Q. Yuan (2021), 2104.03274.

[24] M. Van Beekveld, W. Beenakker, M. Schutten, and J. De Wit (2021), 2104.03245.

[25] P. Cox, C. Han, and T. T. Yanagida (2021), 2104.03290.

[26] F. Wang, L. Wu, Y. Xiao, J. M. Yang, and Y. Zhang (2021), 2104.03262.

[27] Y. Gu, N. Liu, L. Su, and D. Wang (2021), 2104.03239.

[28] J. Cao, J. Lian, Y. Pan, D. Zhang, and P. Zhu (2021), 2104.03284.

[29] W. Yin (2021), 2104.03259.

[30] C. Han (2021), 2104.03292.

[31] A. Aboubrahim, M. Klasen, and P. Nath (2021), 2104.03839.

[32] J.-L. Yang, H.-B. Zhang, C.-X. Liu, X.-X. Dong, and T.-F. Feng (2021), 2104.03542.

[33] M. Chakraborti, L. Roszkowski, and S. Trojanowski (2021), 2104.04458.

[34] P. M. Ferreira, B. L. Gonçalves, F. R. Joaquim, and M. Sher (2021), 2104.03367.

[35] H.-X. Wang, L. Wang, and Y. Zhang (2021), 2104.03242.

[36] T. Li, J. Pei, and W. Zhang (2021), 2104.03334.

[37] M. Cadeddu, N. Cargioli, F. Dordei, C. Giunti, and E. Picciau (2021), 2104.03280.

[38] L. Calibbi, M. L. López-Ibáñez, A. Melis, and O. Vives (2021), 2104.03296.

[39] J. Chen, Q. Wen, F. Xu, and M. Zhang (2021), 2104.03699.

[40] P. Escribano, J. Terol-Calvo, and A. Vicente (2021), 2104.03705.

[41] E. J. Chun and T. Mondal (2021), 2104.03701.

[42] G. Arcadi, A. S. De Jesus, T. B. De Melo, F. S. Queiroz, and Y. S. Villamizar (2021), 2104.04456.

[43] C.-H. Chen, C.-W. Chiang, and T. Nomura (2021), 2104.03275.

[44] T. Nomura and H. Okada (2021), 2104.03248.

[45] P. Athron, C. Balázs, D. H. Jacob, W. Kotlarski, D. Stöckinger, and H. Stöckinger-Kim (2021), 2104.03691.

[46] R. Aaij et al. (LHCb) (2021), 2103.11769.

[47] E. Aprile et al. (XENON) (2020), 2006.09721.

[48] F. Takahashi, M. Yamada, and W. Yin, Phys. Rev. Lett. **125**, 161801 (2020), 2006.10035.

[49] G. Alonso-Álvarez, F. Ertas, J. Jaeckel, F. Kahlhoefer, and L. J. Thormaehlen (2020), 2006.11243.

[50] K. Kannike, M. Raidal, H. Veermäe, A. Strumia, and D. Teresi (2020), 2006.10735.

[51] B. Fornal, P. Sandick, J. Shu, M. Su, and Y. Zhao, Phys. Rev. Lett. **125**, 161804 (2020), 2006.11264.

[52] M. Du, J. Liang, Z. Liu, V. Q. Tran, and Y. Xue (2020), 2006.11949.

[53] P. Ko and Y. Tang (2020), 2006.15822.

[54] L. Su, W. Wang, L. Wu, J. M. Yang, and B. Zhu (2020), 2006.11837.

[55] K. Harigaya, Y. Nakai, and M. Suzuki (2020), 2006.11938.

[56] D. Borah, S. Mahapatra, D. Nanda, and N. Sahu (2020), 2007.10754.

[57] D. Choudhury, S. Maharana, D. Sachdeva, and V. Sahdev (2020), 2007.08205.

[58] J. Bramante and N. Song, Phys. Rev. Lett. **125**, 161805 (2020), 2006.14089.

[59] N. F. Bell, J. B. Dent, B. Dutta, S. Ghosh, J. Kumar, and J. L. Newstead, Phys. Rev. Lett. **125**, 161803 (2020), 2006.12461.

[60] D. Borah, S. Mahapatra, and N. Sahu (2020), 2009.06294.

[61] A. Aboubrahim, M. Klasen, and P. Nath (2020), 2011.08053.

[62] H. M. Lee (2020), 2006.13183.

[63] S. Baek, J. Kim, and P. Ko, Phys. Lett. B **810**, 135848 (2020), 2006.16876.

[64] S. Shakeri, F. Hajkarim, and S.-S. Xue, Journal of High Energy Physics **2020** (2020), ISSN 1029-8479, URL http://dx.doi.org/10.1007/JHEP12(2020)194.

[65] A. Bally, S. Jana, and A. Trautner, Phys. Rev. Lett. **125**, 161802 (2020), 2006.11919.

[66] L. Delle Rose, G. Hütsi, C. Marzo, and L. Marzola (2020), 2006.16078.

[67] Y. Ema, F. Sala, and R. Sato (2020), 2007.09105.

[68] M. Dutta, S. Mahapatra, D. Borah, and N. Sahu (2021), 2101.06472.

[69] M. Baryakhtar, A. Berlin, H. Liu, and N. Weiner (2020), 2006.13918.

[70] W. Chao, Y. Gao, and M. j. Jin (2020), 2006.16145.

[71] H. An and D. Yang (2020), 2006.15672.

[72] H.-J. He, Y.-C. Wang, and J. Zheng (2020), 2007.04963.

[73] J. Kim, T. Nomura, and H. Okada, Phys. Lett. B **811**, 135862 (2020), 2007.09894.

[74] W.-Y. Keung, D. Marfatia, and P.-Y. Tseng (2020), 2009.04444.

[75] H.-J. He, Y.-C. Wang, and J. Zheng (2020), 2012.05891.

[76] S.-M. Choi, H. M. Lee, and B. Zhu (2020), 2012.03713.

[77] D. McKeen, M. Pospelov, and N. Raj (2020), 2006.15140.

[78] Y. Jho, J.-C. Park, S. C. Park, and P.-Y. Tseng (2020), 2006.13910.

[79] H. Alhazmi, D. Kim, K. Kong, G. Mohlabeng, J.-C. Park, and S. Shin (2020), 2006.16252.

[80] A. Das and M. Sen (2021), 2104.00027.

[81] X. He, G. C. Joshi, H. Lew, and R. Volkas, Phys. Rev. D **43**, 22 (1991).

8

[82] X.-G. He, G. C. Joshi, H. Lew, and R. R. Volkas, Phys. Rev. D **44**, 2118 (1991).

[83] D. Kim, J.-C. Park, and S. Shin, Phys. Rev. Lett. **119**, 161801 (2017), 1612.06867.

[84] G. F. Giudice, D. Kim, J.-C. Park, and S. Shin, Phys. Lett. B **780**, 543 (2018), 1712.07126.

[85] A. Biswas and A. Shaw, JHEP **05**, 165 (2019), 1903.08745.

[86] S. Patra, S. Rao, N. Sahoo, and N. Sahu, Nucl. Phys. B **917**, 317 (2017), 1607.04046.

[87] S. J. Brodsky and E. De Rafael, Phys. Rev. **168**, 1620 (1968).

[88] S. Baek and P. Ko, JCAP **10**, 011 (2009), 0811.1646.

[89] F. S. Queiroz and W. Shepherd, Phys. Rev. D **89**, 095024 (2014), 1403.2309.

[90] G. Belanger and J.-C. Park, JCAP **1203**, 038 (2012), 1112.4491.

[91] F. D'Eramo and S. Profumo, Phys. Rev. Lett. **121**, 071101 (2018), 1806.04745.

[92] B. Roberts and V. Flambaum, Phys. Rev. D **100**, 063017 (2019), 1904.07127.

[93] K. Griest and D. Seckel, Nucl. Phys. B **283**, 681 (1987), [Erratum: Nucl.Phys.B 296, 1034–1036 (1988)].

[94] A. Gould, Astrophys. J. **321**, 560 (1987).

[95] A. Abdelhameed et al. (CRESST), Phys. Rev. D **100**, 102002 (2019), 1904.00498.

[96] W. Altmannshofer, S. Gori, M. Pospelov, and I. Yavin, Phys. Rev. Lett. **113**, 091801 (2014), 1406.2332.

[97] D. Akimov et al. (COHERENT), Science **357**, 1123 (2017), 1708.01294.

[98] D. Akimov et al. (COHERENT), Phys. Rev. Lett. **126**, 012002 (2021), 2003.10630.

[99] M. Cadeddu, N. Cargioli, F. Dordei, C. Giunti, Y. F. Li, E. Picciau, and Y. Y. Zhang, JHEP **01**, 116 (2021), 2008.05022.

[100] H. Banerjee, B. Dutta, and S. Roy (2021), 2103.10196.

[101] J. Lees et al. (BaBar), Phys. Rev. D **94**, 011102 (2016), 1606.03501.

[102] M. Bauer, P. Foldenauer, and J. Jaeckel, JHEP **18**, 094 (2020), 1803.05466.

[103] A. Kamada, K. Kaneta, K. Yanagi, and H.-B. Yu, JHEP **06**, 117 (2018), 1805.00651.

[104] N. Aghanim et al. (Planck) (2018), 1807.06209.

[105] M. Ibe, S. Kobayashi, Y. Nakayama, and S. Shirai, JHEP **04**, 009 (2020), 1912.12152.

[106] M. Escudero, D. Hooper, G. Krnjaic, and M. Pierre, JHEP **03**, 071 (2019), 1901.02010.

[107] N. Sabti, J. Alvey, M. Escudero, M. Fairbairn, and D. Blas, JCAP **01**, 004 (2020), 1910.01649.

[108] G. Krnjaic, G. Marques-Tavares, D. Redigolo, and K. Tobioka, Phys. Rev. Lett. **124**, 041802 (2020), 1902.07715.

[109] S. Gninenko, N. Krasnikov, and V. Matveev, Phys. Rev. D **91**, 095015 (2015), 1412.1400.

[110] S. Gninenko and N. Krasnikov, Phys. Lett. B **783**, 24 (2018), 1801.10448.

[111] P. Gondolo and G. Gelmini, Nucl. Phys. **B360**, 145 (1991).